The Behavior of Exciplex Decay Processes and Interplay of Radiationless Transition and Preliminary Reorganization Mechanisms of Electron Transfer in Loose and Tight Pairs of Reactants

Michael G. Kuzmin,* Irina V. Soboleva, and Elena V. Dolotova

Department of Chemistry, Moscow State Lomonosov University, Moscow, 119992, Russia

Received: September 28, 2006; In Final Form: October 31, 2006

Exciplex emission spectra and rate constants of their decay via internal conversion and intersystem crossing are studied and discussed in terms of conventional radiationless transition approach. Exciplexes of 9-cyanophenanthrene with 1,2,3-trimethoxybenzene and 1,3,5-trimethoxybenzene were studied in heptane, toluene, butyl acetate, dichloromethane, butyronitrile, and acetonitrile. A better description of spectra and rate constants is obtained using 0−0 transition energy and Gauss broadening of vibrational bands rather than the free energy of electron transfer and reorganization energy. The coincidence of parameters describing exciplex emission spectra and dependence of exciplex decay rate constants on energy gap gives the evidence of radiationless quantum transition mechanism rather than thermally activated medium reorganization mechanism of charge recombination in exciplexes and excited charge transfer complexes (contact radical ion pairs) as well as in solvent separated radical ion pairs. Radiationless quantum transition mechanism is shown to provide an appropriate description also for the main features of exergonic excited-state charge separation reactions if fast mutual transformations of loose and tight pairs of reactants are considered. In particular, very fast electron transfer (ET) in tight pairs of reactants with strong electronic coupling of locally excited and charge transfer states can prevent the observation of an inverted region in bimolecular excited-state charge separation even for highly exergonic reactions.

Introduction

The problem of exciplex decay rates is a crucial point for the transient exciplex mechanism of excited-state electron transfer.[1−8] Radiationless decay of exciplexes via internal conversion and intersystem crossing can be considered as charge recombination (CR) yielding ground or triplet states of contact pair of reactants.[9−11] Thus, they should follow either the mechanism of thermally activated preliminary reorganization of medium and reactants (original Marcus model[12] later was extended to radiationless transition mechanism by Marcus[9] and other authors[13,14]) or the radiationless quantum transition mechanism.[12−17] To find out the actual mechanism of exciplex decay, we compare the experimentally obtained parameters for exciplex emission with those for exciplex decay because emission and radiationless decay are expected to have close parameters due to similar physical behavior of radiative and radiationless quantum transition mechanisms. This comparison demonstrates that exciplex decay indeed follows radiationless quantum transition mechanism rather than thermally activated ET reactions mechanism. A consideration of competition of these two mechanisms with a distinct physical behavior seems to be more reasonable, explicit, and valid than the excessive complication of some "unified" models. A competition of two mechanisms implies a transformation of the actual dominating mechanism as a function of the driving force and other factors.

The difference between CR rates in exciplexes (and contact radical ion pairs, CRIPs) and in solvent separated radical ion pairs (SSRIPs) can be attributed to greater electronic coupling and smaller medium reorganization energy for exciplexes and CRIPs relative to SSRIPs.[18−32] The amplitude of the maximum of CR rate constant−free energy dependence is determined by the value of the matrix element, and the position of the maximum along the free energy axis is governed by reorganization energy. Finally, a model of competition of radiationless and thermally activated reorganization mechanisms in contact (or tight) pairs (TP) and in solvent separated (or loose) pairs (LP) of reactants is extended to charge separation (CS) reactions. Such a model is found to provide the appropriate description for the main features of exergonic excited-state CS reactions when fast mutual transformations of LP and TP are considered. In particular, the absence of the inverted region in bimolecular CS reactions can be attributed to the very fast CS in TP of reactants due to strong electronic coupling of locally excited and charge transfer states.

Experimental Section

Electron acceptor 9-cyanophenanthrene (CP, $E(A/A^-) = -1.91$ V, $E^* = 3.42$ eV) (Aldrich, 98%) and electron donors 1,2,3-trimethoxybenzene (123TMB, $E(D^+/D) = 1.42$ V) (Janssen Chimica, 98%) and 1,3,5-trimethoxybenzene (135TMB, $E(D^+/D) = 1.49$ V) (Aldrich, 99%) were used without additional purification. Heptane (C_6H_{14}, $\epsilon_S = 1.924$), toluene ($PhCH_3$, $\epsilon_S = 2.379$), butyl acetate (AcOBu, $\epsilon_S = 5.01$), dichloromethane (CH_2Cl_2, $\epsilon_S = 9.08$), butyronitrile (PrCN, $\epsilon_S = 20.3$), and acetonitrile (MeCN, $\epsilon_S = 37.5$) were distilled prior to use. Here, $E(D^+/D)$ and $E(A/A^-)$ are redox (polarographic) potentials of electron donor and electron acceptor in acetonitrile, E^* is the energy of the acceptor excitation ($E^* = h\nu_0$, where ν_0 is a frequency of 0−0 transition in the acceptor), and ϵ_S is the solvent dielectric permittivity.

* Corresponding author. E-mail: kuzmin@photo.chem.msu.ru.

10.1021/jp066379e CCC: $37.00
Published on Web 12/19/2006

The absorption and emission spectra were recorded on a Shimadzu UV-2101PC spectrophotometer and a Perkin-Elmer LS-50 spectrofluorimeter. The excitation wavelength corresponded to the long-wavelength absorption maximum of an acceptor in a given solvent. The acceptor concentration was about 10^{-5} M and that of a quencher was varied in the range 0.01−0.4 M. All measurements of emission spectra were carried out in outgassed solutions using four cycles of the freeze−pump−thaw technique at a pressure of about 0.01 Pa. The procedures of isolation of the emission spectra of the excited acceptors and exciplexes, approximation of the emission spectra with the asymmetric Gauss function, determination of average emission frequency, $h\nu'_{Av}$, absolute quantum yields of fluorescence, internal conversion, intersystem crossing and ion-radical formation in exciplexes (φ'_F, φ'_{IC}, φ'_{ISC}, and φ'_R), and the values of exciplexes lifetimes τ'_0 and rate constants of internal conversion and intersystem crossing (k_{IC}' and k_{ISC}') for exciplexes of CP were described elsewhere.[33−37]

The value of free energy of ground-state electron transfer ΔG_{ET} in acetonitrile was calculated as

$$\Delta G_{ET} = E(D^+/D) - E(A/A^-) \quad (1)$$

Results and Discussion

Exciplex Emission Spectra. Exciplex emission spectra provide the most direct information on the values of vertical energy gap between singlet excited and ground states $\Delta E_{CR} = h\nu'_0$ and other parameters, which are necessary for the discussion of the behavior of radiationless transition. Obtained exciplex emission spectra (as a function of a number of photons per unit frequency interval vs energy of emitted photon $h\nu'$) were fit to the equation[14]

$$(I(\nu')/\nu')/I_0 = \sum_m [\exp(-S)(S^m/m!)] \times \exp[-(h\nu'_0 - h\nu' - m\, h\nu_V)^2/2\sigma^2] \quad (2)$$

This equation represents the emission band as a sum of vibronic transitions with Gaussian bandshapes. Here ν'_0 is a frequency of 0−0 transition, $S = \lambda_v/h\nu_V$ is the Huang−Rhys spectral factor,[38] λ_V is the internal reorganization energy associated with the dominant (or average) high-frequency vibration mode (quantum accepting mode in contrast to classic internal reorganization energy λ_i), ν_V is a vibrational frequency of this mode, and σ is a width of the vibronic bands. This expression is completely equivalent mathematically to another expression commonly used by many authors [9,11,30−32,39] for charge transfer (CT)-transitions

$$I(\nu')/\nu' = (64\pi^4 n^3/3h^3c^3)V_{10}^2(\Delta\mu)^2(4\pi\lambda_0 k_B T)^{-1/2} \times \sum_m [\exp(-S)(S^m/m!)] \exp[-(\Delta G_{CR} + \lambda_0 + h\nu' + m\, h\nu_V)^2/4\lambda_0 k_B T] \quad (3)$$

if the energy gap between the charge transfer state and the ground (G) states $\Delta E_{CR} = h\nu'_0 = -(\Delta G_{CR} + \lambda_0)$ and $\sigma^2 = 2\lambda_0 k_B T$. Here V_{10} is the matrix element coupling charge transfer and ground states, $\Delta G_{CR} = -\Delta G_{ET}$, $\Delta\mu$ is the difference in dipole moment between these states, and λ_0 is the reorganization energy of solvent and other low frequency (classical) modes. But the physical nature of these expressions is quite different. Equation 2 corresponds to the spectral envelope formed by Gauss broadening of the vibronic levels. Equation 3 in fact attributes the broadening of the vibronic bands to thermal fluctuations of the medium reorganization in the initial state solely. Inhomogeneous broadening of vibronic levels, typical for liquids and solids, is caused by various kinds of intermolecular interactions besides the medium reorganization. Therefore σ is related also to many other factors and its value should exceed $(2\lambda_0 k_B T)^{1/2}$. In contrast, the energy gap ΔE_{CR} and the energy of the 0−0 transition, $h\nu'_0$, are related directly to the medium reorganization energy (Chart 1). The separation of σ and λ_0 provides more correct description of the exciplex emission spectra.

CHART 1

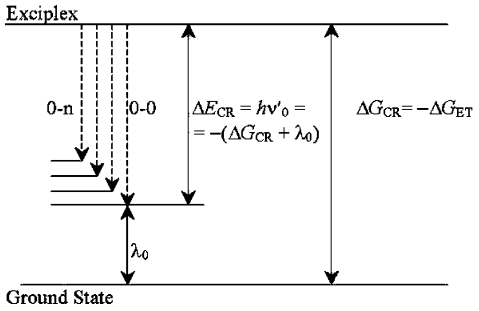

Figure 1 presents an example of the emission spectrum of CP−123TMB exciplex in butyl acetate at room temperature and the results of its fitting to eq 2. In a preliminary fitting, $h\nu_V$ and S were adjusted as 0.2 eV and 1.5, respectively, which are typical values for exciplexes,[31] and $h\nu'_0$ and σ were varied to obtain optimal coincidence of experimental and simulated spectra. To refine the fitting procedure, all four parameters were varied. It was found that variations of σ affected the spectra envelope very weakly if $\sigma > 0.1$ eV. The obtained data on values of $h\nu'_0$, $h\nu_V$, S, and σ for CP−123TMB and CP−135TMB exciplexes in various solvents are summarized in Table 1. Variations of the parameters $h\nu_V$ and S for both exciplexes of CP with the solvent polarity are rather small. This provides a possibility to consider these parameters as constants in further analysis of radiationless decay rate constants.

Gould already noted[31] that fitting of eq 3 to experimental emission spectra provided values of the sum $(\Delta G_{CR} + \lambda_0) = -\Delta E_{CR} = -h\nu'_0$ with much better accuracy than that of ΔG_{CR} and λ_0 separately. In combined fitting to absorption and emission spectra, Stokes shift dominates in the determination of λ_0, and the obtained values of λ_0 can differ from $\sigma^2/2k_BT$. The individual fitting to absorption and emission spectra provides the value of $\lambda_0 = \sigma^2/2k_BT$ because the spectral envelope is defined by the width of vibronic bands, and information on actual reorganization energy is missed. This indicates that inhomogeneous broadening substantially exceeds the medium reorganization broadening. Radiationless and radiative transitions probability depends on quantum coordinates and related parameters h_V, λ_V, σ, and ΔE_{CR} rather than on classic coordinates and parameters λ_0 and ΔG_{CR}. Thus the values of ΔG_{CR} and λ_0, obtained from combined fitting of absorption and emission spectra, are inapplicable for the evaluation of radiationless or radiative decay parameters.

According to Chart 1, a shift of $h\nu'_0$ in a given solvent relative to some nonpolar reference solvent is equal to the difference of their reorganization energies $h\nu'_0(R) - h\nu'_0(S) = \lambda_0(S) - \lambda_0(R)$. But the experimental data, obtained for the exciplex CP−135TMB (Table 2), show that the difference in energies of 0−0 transition in a given solvent and heptane is markedly lower than the corresponding difference in values of $\sigma^2/2k_BT$, especially in polar solvents. This means that spectral broadening and spectral shift have different origin. A similar difference between

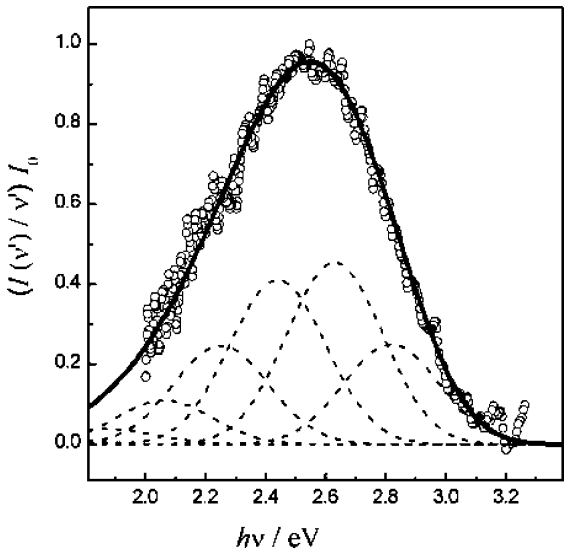

Figure 1. Emission spectrum of CP−123TMB exciplex in butyl acetate at room temperature and the results of its fitting to eq 2. Contributions of 0−0, 0−1, 0−2, 0−3, 0−4, 0−5, and 0−6 vibronic transitions are shown by dash lines.

TABLE 1: Spectral and Kinetic Parameters of Exciplexes CP−123TMB and CP−135TMB

exciplex	CP−123TMB			CP−135TMB		
	$PhCH_3$	AcOBu	PrCN	$PhCH_3$	AcOBu	PrCN
τ_0'/ns[a]	20	6	2.3	27.4	32	14
φ_F'[b]	0.21	0.12	0.01	0.21	0.18	0.08
φ_{ISC}'[c]	0.53	0.25	0.16	0.42	0.42	0.35
φ_R'[d]	0	0	0.18	0	0	0.20
φ_{IC}'[e]	0.26	0.63	0.65	0.37	0.40	0.37
$k_F'/\mu s^{-1}$[f]	11	20	4	8	6	6
$k_{ISC}'/\mu s^{-1}$[g]	26	42	70	15	13	25
$k_{IC}'/\mu s^{-1}$[h]	13	105	283	14	12	26
$(U_{CT}^0-U_{LE}^0)$/eV[i]	−0.55	−0.55	−0.55	−0.13	−0.13	−0.13
V_{12}/eV[j]	0.2	0.2	0.2	0.2	0.2	0.2
$(\mu_0^2/\rho^3)(e^2/4\pi\epsilon_0)$ /eV[k]	0.5	0.5	0.5	0.8	0.8	0.8
z[l]	0.93	0.95	0.96	0.76	0.87	0.93
$h\nu'_0$/eV[m]	2.92	2.81	2.64	3.24	3.15	2.94
σ/eV[n]	0.12	0.16	0.13	0.10	0.11	0.17
S[o]	1.9	2.0	1.9	1.9	1.9	1.9
$h\nu_V$/eV[p]	0.19	0.19	0.20	0.19	0.20	0.20
$\sigma^2/(2k_BT)$/eV	0.29	0.51	0.34	0.20	0.24	0.58
ΔE_{ST}/eV[q]	0.31	0.21	0.15	0.63	0.48	0.31

[a] Lifetime of exciplex. [b]Quantum yield of exciplex emission. [c]Quantum yield of triplets. [d]Quantum yield of radical ions. [e]Quantum yield of exciplex internal conversion. [f]Emission rate constant. [g]Intersystem crossing rate constant. [h]Internal conversion rate constant. [i]Difference in energies of CT and LE states of reactant pair in vacuum. [j]Matrix element coupling charge transfer (CT) and singlet (LE) state. [k]μ_0 is the dipole moment of CT state and ρ is the radius of the solvent cavity, containing the exciplex. [l]Degree of charge transfer in exciplex. [m]Energy of 0−0-transition. [n]Gauss broadening of vibronic band. [o]Spectral Huang−Rhys factor. [p]Energy of the dominant high-frequency vibration. [q]Difference in energy of 0−0 transition in exciplex and energy of local triplet state.

spectral broadening and spectral shift was observed also for absorption spectra of betains in various solvents.[14]

Common Marcus expression for solvent reorganization energy, which considers the solvation energy of two oppositely charged ions in SSRIP,[12]

$$\lambda_S = (e^2/4\pi\epsilon_0)(1/2\rho_A + 1/2\rho_D - 1/r_{AD})(1/n^2 - 1/\epsilon_S) \quad (4)$$

is not valid for exciplexes or CRIPs. Figure 2 presents the

TABLE 2: Energies of 0−0 Transition $h\nu'_0$ and Spectral Broadening σ for Emission Spectra of CP−135TMB Exciplex in Various Solvents[a]

solvent	$h\nu'_0$/eV	σ/eV	$h\nu'_0$ (R) − $h\nu'_0$ (S))/eV	$(\sigma(S))^2/2k_BT$ − $(\sigma(R))^2/2k_BT$/eV
heptane	3.24	0.08	0	0
toluene	3.24	0.1	0.00	0.07
butyl acetate	3.15	0.11	0.09	0.11
butyronitrile	2.94	0.17	0.30	0.45
acetonitrile	2.86	0.19	0.38	0.59

[a] Heptane is used as a reference solvent R.

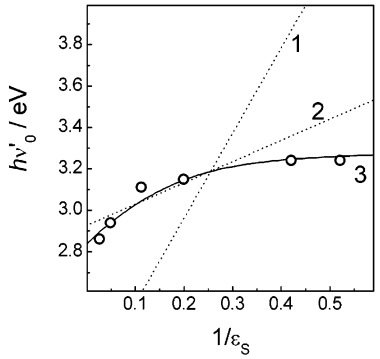

Figure 2. Experimental dependence of $h\nu'_0$ on $1/\epsilon_S$ obtained for CP−135TMB exciplex (circles), calculated dependences $h\nu'_0$ on $1/\epsilon_S$ according to the model of two ions (eq 6) with $r_{AD} = 0.7$ and 0.4 nm (dash lines 1 and 2, respectively), and the model of selfconsistent polarization of the medium and exciplex (eq 8) (line 3).

dependence of experimental value of $h\nu'_0$ on $1/\epsilon_S$ obtained for CP−135TMB exciplex and calculated dependences $h\nu'_0 = (\Delta G_{ET}(S) - \lambda_S)$ on $1/\epsilon_S$ (lines 1 and 2) according to eqs 4, 5:

$$\Delta G_{ET}(S) = \Delta G_{ET}(R) + (e^2/4\pi\epsilon_0) \times [(1/2\rho_A + 1/2\rho_D) \times (1/\epsilon_S - 1/\epsilon_R) - 1/(\epsilon_S r_{AD})] \quad (5)$$

where $\Delta G_{ET}(S)$ and $\Delta G_{ET}(R)$ are ΔG_{ET} in a solvent S and a reference solvent R (usually MeCN).

$$h\nu'_0 = \Delta G_{ET}(S) - \lambda_S = \Delta G_{ET}(R) + (e^2/4\pi\epsilon_0)[(2/\epsilon_S)(1/\rho_{A(D)} - 1/r_{AD}) + (1/n^2)(1/r_{AD} - 1/\rho_{A(D)} - 1/\rho_{A(D)}\epsilon_R)] \quad (6)$$

where n is the refractive index of the solvent, ϵ_S and ϵ_R are the dielectric permittivity of the given and reference solvents, $4\pi\epsilon_0$ is the vacuum permittivity ($(e^2/4\pi\epsilon_0) = 1.44$ eV nm), and r_{AD} and $\rho_{A(D)}$ are the center-to-center distance between reactants and solvent shell radii, respectively (assuming $\rho_A \approx \rho_D$). It is supposed frequently that $\lambda_0 \approx \lambda_S$ (i.e., the main contribution into total classic reorganization energy λ_0 is provided by the energy of medium reorganization λ_S) and classic internal reorganization energy λ_i is neglected.

The slope of the dependence, calculated by eq 6 with usually used values $r_{AD} = 0.7$ nm and $\rho_{A(D)} = 0.35$ nm (Figure 2, line 1) is several times larger than that of the experimental one. Better coincidence of the slopes of experimental and calculated dependences can be obtained if one uses substantially smaller values of $r_{AD} \approx 0.4$ nm $< (\rho_A+\rho_D)$ (Figure 2, line 2). This contradicts the common model of ions solvation, but 0.4 nm is quite a realistic value for the center-to-center distance between reactants for sandwich-type exciplexes and corresponds better to the structure of exciplexes than of SSRIPs. Similar dependences were observed for CP−123TMB exciplex.

Another approach[37,40,41] considering selfconsistent polarization of the medium by electric dipole of the exciplex with variable degree of charge transfer (z) gives better agreement of spectral shifts and reorganization energies with the medium permittivity

$$U_{LE}^{0} - U_{CT}^{0} = V_{12}[1/(1/z-1)^{1/2} - (1/z-1)^{1/2}] - 2z(e^2/4\pi\epsilon_0)(\mu_0^2/\rho^3)\, f(\epsilon) \quad (7)$$

Here U_{LE}^0 and U_{CT}^0 are energies of LE and CT states of the reactant pair in vacuum, V_{12} corresponds to CT and LE states, μ_0 and ρ are the dipole moment of CT state and the radius of the solvent cavity, containing the exciplex, respectively, $(e^2/4\pi\epsilon_0)(\mu_0^2/\rho^3) = 0.7 - 1.2$ eV,[37,40-44] $f(\epsilon) = (\epsilon-1)/2(\epsilon+2)$, and $f(n^2) = (n^2-1)/2(n^2+2)$.[41] This approach yields (in Franck−Condon approximation)

$$h\nu'_0 = U_{CT}^{0} - z[2f(\epsilon) - z\, f(n^2)](e^2/4\pi\epsilon_0)(\mu_0^2/\rho^3) - V_{12}(1/z-1)^{1/2} \quad (8)$$

This expression includes a degree of charge transfer z, which can be expressed in implicit form as

$$f(\epsilon) = \{(U_{LE}^{0} - U_{CT}^{0}) - V_{12}[(1/z-1)^{1/2} - 1/(1/z-1)^{1/2}]\}/[2z(e^2/4\pi\epsilon_0)(\mu_0^2/\rho^3)] \quad (9)$$

Curve 3 in Figure 2 presents, according to eq 8, simulated dependence $h\nu'_0$ vs $1/\epsilon$ for CP−135TMB exciplex, which describes adequately the experimental data. In this approach solvent reorganization energy for exciplexes and CRIPs can be expressed as

$$\lambda s' = V_{12}(1/z-1)^{1/2} + (e^2/4\pi\epsilon_0)\, f(\epsilon)(\mu_0^2/\rho_{AD}^3)\, z(2-z)[f(n^2) - f(\epsilon_S)] \quad (10)$$

When the energy gap between LE and CT states is large enough ($(U_{LE}^0 - U_{CT}^0) > 2V_{12}$) (in CRIPs), $z \approx 1$ and

$$\lambda s' \approx (e^2/4\pi\epsilon_0)(\mu_0^2/\rho_{AD}^3)[f(n^2) - f(\epsilon_S)] \quad (11)$$

Direct measurements of rate constants and equilibrium constants of forward and backward conversion of contact into solvent separated geminate radical ion pairs[45,46] formed from tetracyanobenzene with methylbenzenes confirms also that eq 4 overestimates values of λ_S for CRIPs. In polar solvents (PrCN and BuCN), the experimental value of the difference ΔG(CRIP) − ΔG(SSRIP) is rather small (ca. −0.03 eV), whereas for nonpolar solvents with $\epsilon = n^2$ this difference reaches 0.4 eV and corresponds to vertical Franck−Condon transition. Reorganization energies for these CRIPs and SSRIPs in nitriles are ca. 0.4 and 0.8 eV, respectively. The value ΔG(CRIP→SSRIP) is practically independent of ΔG_{ET}* (slope <0.03) but strongly depends on $1/\epsilon_S$ and/or on $f(\epsilon_S)$ with the slopes ca. 1.0 eV. This indicates the increase of the distances r_{AD} on ca. 0.2−0.3 nm or trebling of (μ^2/ρ^3) (the increase of μ ca. 1.5 times) in SSRIPs relative to CRIPs. Several times smaller values of the reorganization energy for exciplexes and CRIPs relative to SSRIPs have important consequences for rates of their decay and charge recombination.

It should be emphasized that values of $h\nu'_0 = \Delta E_{CR}$ can be obtained with much better accuracy than the value of ΔG_{CR} calculated from electrochemical data. It is reasonable to use actual vertical energy gap $h\nu'_0$ in further analysis of rate constants.

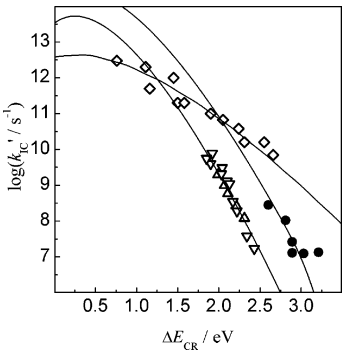

Figure 3. Plots of internal conversion rate constants k_{IC}' vs ΔE_{CR} for exciplexes CP−123TMB and CP−135TMB (●) in various solvents, TCNB with various alkylbenzenes (△) in chloroform and with hexamethylbenzene (▽) in various solvents,[31] TCNE, PMDA, and PA with arenes (◇) in MeCN[47] and their fitting to eq 12 with parameters given in Table 3.

Experimental Dependence of CR Rate Constants on the Energy Gap In Exciplexes. We studied the dependence of rate constants of internal conversion (IC) and intersystem crossing (ISC) on the energy gap to analyze the validity of radiationless quantum transitions mechanism to the processes of charge recombination in exciplexes and other radical-ion pairs.

The dependence of rate constants of ET by radiationless mechanism is described by the following equation:

$$k_{ET} = (4\pi^2/h)V^2[1/\sigma(2\pi)^{1/2}] \sum_m [\exp(-S)(S^m/m!)] \times \exp[-(\Delta E_{ET} - m\, h\nu_V)^2/2\sigma^2] \quad (12)$$

which corresponds to radiationless transition with Gauss broadening of vibronic bands. Here V is a matrix element coupling initial and final states. The fitting of this equation to experimental dependence of k_{ET} on $h\nu'_0 = \Delta E_{ET} = \Delta E_{CR}$ yields four parameters: V, σ, S, and $h\nu_V$ and can be used for the analysis of data in various solvents, because all these parameters are practically independent of solvent polarity.

Figure 3 demonstrates the dependences of experimental values of rate constants k_{IC}' on ΔE_{CR} for exciplexes of 9-cyanophenanthrene with methoxybenzenes (our data) and 1,2,4,5-tetracyanobenzene (TCNB) with alkylbenzenes (data from ref 31) in various solvents and CRIPs of tetracyanoethylene (TCNE), pyromellite dianhydride (PMDA), and phthalyc anhydride (PA) with arenes (data from ref 47) in MeCN. These dependences were fitted to eq 12 ($k_{ET} \equiv k_{IC}'$, $\Delta E_{ET} \equiv \Delta E_{CR}$, $V \equiv V_{10}$). We used the value of $h\nu'_0$ as ΔE_{CR} for exciplexes of CP. We used the sum ($\Delta G_{CR} + \lambda_S$) obtained by the authors by fitting of the exciplex emission and absorption spectra to eq 3 as the energy gap for data of Gould et al.[31] For the data of Mataga et al.[47] the energy gap was calculated as $\Delta E_{CR} = h(\nu^a_{max} + \nu^f_{max})/2 \approx -\Delta G_{IP} + 0.2$ eV in which ν^a_{max} and ν^f_{max} were authors' data on maxima of absorption and emission spectra of CT complexes, and ΔG_{IP} was the free energy gap between the contact ion pair and ground state. In the Figure 3 charge recombination IC rate constants for exciplexes and CRIPs decrease with the increase of ΔE_{CR}. That is, only the so-called "inverted region" is observed for charge recombination in exciplexes and CRIPs. Obtained values of parameters V_{10}, σ, S, λ_V, and $h\nu_V$ are given in Table 3. Parameters σ, S, and $h\nu_V$ obtained for CP exciplexes from spectral and kinetic (Table 1) data are reasonably close to each other. It is significant that for CP exciplexes the value of V_{10} is practically equal to the value of V_{12}, ca. 0.2 eV, obtained earlier[37] from the dependence of the spectral shift of exciplex average emission frequency relative to that of fluorophore. Value of V_{10}

TABLE 3: Fitting Parameters of eq 12 for Dependences of k_{IC}' on ΔE_{CR} and k_{ISC}'on ΔE_{ST} in Exciplexes, CRIPs and SSRIPs

exciplexes and radical-ion pairs	ΔE_{CR}/ eV[a]	$\log(k_{IC}'/s^{-1})$[b]	V_{10}/ meV	$h\nu_V$/eV	S	λ_V/ eV	σ/ eV	$\sigma^2/(2k_BT)$	λ_S/eV
exciplexes of CP with methoxybenzenes	2.6 − 3.1	7 − 9	150	0.2	2.0	0.4	0.15	0.45	
exciplexes of TCNB with methylbenzenes[c]	1.8 − 2.3	7 − 10	60	0.19	1.7	0.32	0.15	0.45	
excited CT complexes of TCNE, TCNQ, PDA, PA with aromatic hydrocarbons[d]	0.7 − 2.7	10 − 12.7	23	0.4	1.1	0.44	0.2	0.8	0.3
cyanonthracenes, N-methylacridinium cation with methoxybenzenes and alkylanilines[e]	−0.4 − +1.6	10 − 12	10	0.2	2	0.4	0.15	0.45	1.06
DCA and TCA with ethylbenzenes, methylnaphthalenes, and methylanthracenes[f]	0.2 − 1.0	8 − 10.5	1	0.14	2	0.28	0.2	0.8	1.83
TCNE, TCNQ, PMDA, PA with aromatic hydrocarbons[g]	−0.6 − +1.7	8 − 11	2	0.2	2	0.4	0.2	0.8	1.15
Zn-porphyrin−phthalimides dyads[h]	0 − 1	12 − 13	24	0.18	2	0.36	0.12	0.29	0.05

	ΔE_{ST}/ eV [a]	$\log(k_{ISC}'/s^{-1})$ [b]	V_{13}/meV	$h\nu_V$/ eV	S	λ_V/eV	σ/eV	$\sigma^2/(2k_BT)$
CP with methoxybenzenes	0−0.6	7−8	0.06	0.2	0.5	0.1	0.2	0.8
DCA and TCA with methylbenzenes[i]	0−0.9	6−7	0.025	0.2	1.1	0.22	0.2	0.8

[a] The range of the energy gap between CT and ground states ΔE_{CR} and between CT and triplet states ΔE_{ST}. [b]The range of the measured rates. [c]Ref 31. [d]Ref 47. [e]Ref 32. [f]Ref 27. [g]Ref 23. [h]Ref 51. [i]Ref 11.

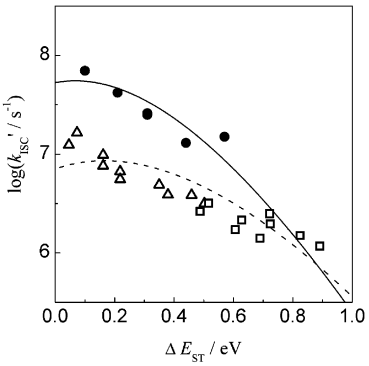

Figure 4. Plots of intersystem crossing rate constants k_{ISC}' vs ΔE_{ST} for exciplexes CP−123TMB and CP−135TMB (●), DCA (□), and TCA (△) with polymethylbenzenes[11] in various solvents and their fitting to eq 12 with parameters given in Table 3.

varies in the range 0.01−0.1 eV for other CRIPs (exciplexes) depending on the chemical nature of parent molecules.

Rate constants of intersystem crossing provide a possibility to follow the dependence of k_{ISC}' on energy gap ΔE_{ST} down to values of ΔE_{ST} that are close to zero. Equation 12 was used for fitting of our and literary data[11] on k_{ISC}' for exciplexes of CP and of 9,10-dicyanoanthracene (DCA) and 2,6,9,10-tetracyanoanthracene (TCA) (Figure 4 and Table 3). The energy gap between singlet and triplet states of exciplex ΔE_{ST} was calculated as a difference in energy of the 0−0 transition in exciplex and the energy of local triplet state.

Close to linear inverted dependence of log k_{ISC}' on ΔE_{ST} is observed down to $\Delta E_{ST} = 0.1$ eV. Values of $h\nu_V$ are found to be close to that for internal conversion, but matrix element coupling CT state and triplet state V_{13} is substantially smaller ($V_{13} \approx (3-6) \times 10^{-5}$ eV) than V_{10} for internal conversion due to spin inversion. Values of S and λ_V are somewhat smaller than that for IC. This suggests substantially smaller perturbations of potential energy surface for intersystem crossing.

Dependences of log k_{CR} on ΔG_{CR} similar to that shown in Figure 3 were observed for various kinds of geminate radical ion pairs (GRIP) by many authors.[18−32] But some complications arise when these GRIPs are generated by excited-state charge separation at high concentration of a quencher (>0.1 mol dm^{-3})[48,49] or by short wavelength excitation of ground-state CT complexes.[50] Ultrafast technique demonstrates strongly nonexponential decay of GRIPs. This is caused by nonstationary effects resulting from rather wide distribution over distances between the radical ions in GRIP and the formation of aggregates with several quencher molecules or by different geometries of ground-state complexes and by faster charge recombination in nonrelaxed state. Only a very minor fraction (<10%) of the ion pair population was found to undergo the slow charge recombination observed in previous investigations. Here we shall discuss only SSRIPs where relatively slow (>1 ps) exponential decay is observed.

In SSRIPs, emission is too weak to be observed experimentally[22−24,26−32] and the value of ΔE_{CR} cannot be determined directly. Usually, the dependence of k_{CR} on ΔG_{CR} is discussed using following equation

$$k_{CR} = (4\pi^2/h)V_{10}^2(4\pi\lambda_S k_B T)^{-1/2}\sum_m[\exp(-S)(S^m/m!)] \times \exp[-(\Delta G_{CR} + \lambda_S + m\,h\nu_V)^2/4\lambda_S k_B T] \quad (13)$$

which provides four parameters: V_{10}, λ_S, S, and $h\nu_V$. Though this expression is completely equivalent mathematically to eq 12 if $h\nu'_0 = -(\Delta G_{CR} + \lambda_S)$ and $\sigma^2 = 2\lambda_S k_B T$, it is applicable in limits of only a single solvent, because it contains the value of the reorganization energy λ_S, which strongly depends on solvent polarity. Besides, one has to take into account the different physical meaning of σ and λ_S. When measurements of k_{CR} are performed in different solvents, their direct comparison as a function of ΔG_{CR} is complicated by different values of λ_S and the lack of proportionality of ΔE_{CR} and ΔG_{CR}. The shift of exciplex emission spectra to longer wavelength and the

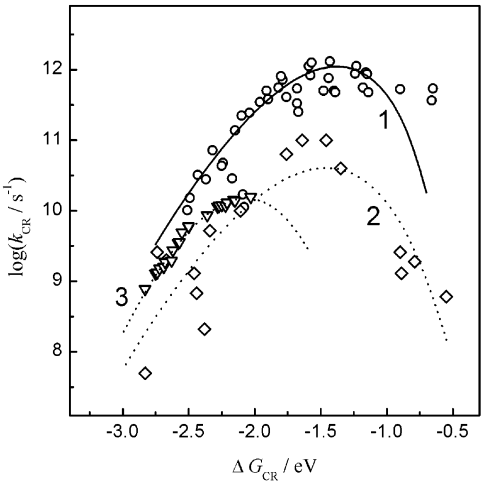

Figure 5. Plots of CR rate constants k_{CR} vs ΔG_{CR} for geminate radical ion pairs formed by excited DCA and TCA with alkylbenzenes (▽),[27] by excited arenes with TCNE, TCNQ, PMDA, PA, and anilines (◇),[23] and by excited cyanoanthracenes and acridinium cation with methoxybenzenes and methylanilines (○)[32] in acetonitrile and their fitting to eq 14. Fitting parameters are given in Table 3.

decrease of $h\nu'_0$ by 0.19−0.20 eV indicate the decrease of ΔE_{CR} and increase of k_{CR} when going from hexane to butyronitrile. This is consistent with the radiationless behavior of the decay when the rate depends on ΔE_{CR} rather than on ΔG_{CR}, and medium reorganization occurs after electron transfer.

Figure 5 presents several examples of the dependences of logk_{CR} on ΔG_{CR} for SSRIPs in acetonitrile. Because no experimental data on the energy gap are available in the publications[23,27,32] for fitting of these data, we used a combination of eqs 12 and 13, assuming $\Delta E_{CR} = -(\Delta G_{CR} + \lambda_S)$

$$k_{CR} = (4\pi^2/h)V_{10}^2[1/\sigma\,(2\pi)^{1/2}] \sum_m [\exp(-S)(S^m/m!)] \times \exp[-(\Delta G_{CR} + \lambda_S + m\,h\nu_V)^2/2\sigma^2] \quad (14)$$

The values of the parameters V_{10}, $h\nu_V$, λ_S, and S, obtained by this way (Table 3), are close to the parameters given in the respective publications. V_{10} is ca. 1−2 orders of magnitude smaller (V_{10} = 0.001−0.003 eV) than V_{10} for exciplexes and CRIPs, suggesting that these geminate pairs are most likely SSRIPs and reflecting substantially greater distance between reactant molecules in such pairs (V_{10} is known to decrease exponentially with the distance). When log k_{CR} is plotted vs ΔG_{CR} the parameter λ_S, in accordance with eq 14, reflects mainly the position of the plot along the ΔG_{CR} axis whereas parameter σ reflects the shape of the plot (its broadening) and has no influence on the position of the plot.

Mataga et al. already discussed the distinctions between rates of charge recombination in CRIPs and SSRIPs formed by reactions of excited arenes with TCNE, TCNQ, PMDA, PA, and anilines[23,47] in terms of different ΔG_{CR} in CRIPs and SSRIPs and the change of the electronic and geometrical structure of the excited CT complex. But a comparison of the plots of log k_{CR} vs ΔE_{CR} for CRIPs and SSRIPs (Figure 6) demonstrates that these distinctions arise mainly from the differences in reorganization energies for CRIPs and SSRIPs. In fact, experimental points for CRIPs and SSRIPs correspond to different ranges of ΔE_{CR}. For CRIPs, all experimental points correspond to $\Delta E_{CR} > \lambda_V$ (0.3 eV) but a part of experimental points for SSRIPs correspond to $\Delta E_{CR} < 0$ in which radiationless transition mechanism fails and only thermally activated reorganization mechanism is possible. Normal dependence of log k_{CR} on ΔG_{CR}

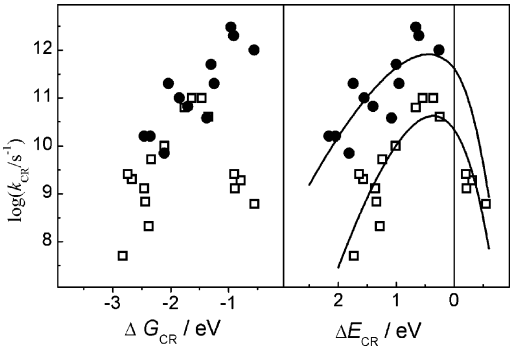

Figure 6. Plots of logk_{CR} vs ΔG_{CR} and ΔE_{CR} for CRIPs (●) and SSRIPs (□) formed by reactions of excited arenes with TCNE, TCNQ, PMDA, PA, and anilines in MeCN.[23,47] $\Delta E_{CR} = -(\Delta G_{CR} + \lambda_S)$, λ_S = 1.0 eV for SSRIPs and 0.5 eV for CRIPs.

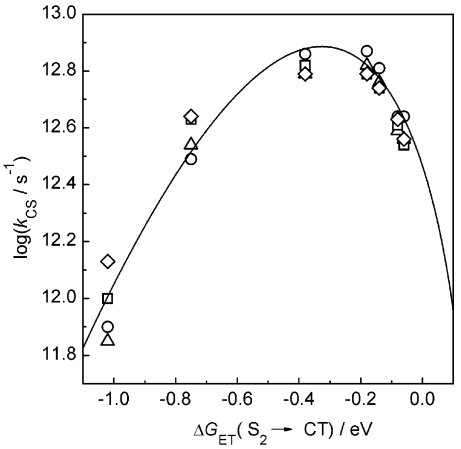

Figure 7. A plot of rate constants of transition from S_2 into CT state in Zn porphyrin-phthalimides dyads in methylcyclohexane (○), toluene (△), tetrahydrofuran (□), and MeCN (◇) vs $\Delta G(S_2 \rightarrow CT)$ in methylcyclohexane.[51]

is inherent in the latter mechanism, whereas inverted dependence is inherent in radiationless transition mechanism at $\Delta E_{CR} > \lambda_V$. This difference between CRIPs and SSRIPs disappears in the plots of log k_{CR} vs ΔG_{CR}, which are close to each other at $\Delta G_{CR} < -1.5$ eV, and differ only at $\Delta G_{CR} > -1.5$ eV in which k_{CR} for SSRIPs starts to decrease.

In the case of ultrafast ET processes when the observed rate constants $k_{ET} > 1/\tau_L \approx 10^{12}$ s^{-1}, it is meaningless to discuss solvent reorganization. The solvent has not managed to respond to the change in the electric field of the ion pair in a time domain of back electron transfer. The energy gap does not change with medium polarity. For instance, Mataga et al. obtained very important experimental results on the rates of the transition from S_2 to CT state (charge separation) in Zn porphyrin−phthalimides dyads.[51] The authors discuss the results in terms of ΔG_{ET} and λ_S although rates of the studied processes (10^{12}−10^{13} s^{-1}) exceed reciprocal values of longitudinal relaxation time τ_L of the solvents used. It becomes obvious that k_{ET} does not depend on the solvent polarity if their data are presented as dependence of logk_{ET} on $\Delta G_{ET}(S_2 \rightarrow CT)$ (Figure 7), where the value of ΔG_{ET}-$(S_2 \rightarrow CT)$ corresponds to methylcyclohexane. Actually, radiationless transition mechanism of ET results in identical dependence of k_{ET} on ΔE_{ET} irrespective of the solvent polarity and evaluated values of ΔG_{ET} and λ_S in the particular solvent because medium reorganization occurs after ET. Thus, the use of the plot of logk_{ET} vs ΔE_{ET} and eq 12 avoids the mistakes related to erroneous consideration of reorganization energies and relaxation processes (explicit or implicit) appearing under investigation of the dependence of logk_{ET} vs ΔG_{ET}. Another

important feature of these data is the identical mechanism of ET in the whole range of ΔE_{ET} studied (ca. 0−1.0 eV). It is confirmed, first, by good quantitative description of experimental data by radiationless quantum transition mechanism by only eq 12 and, second, by the fact that the thermally activated mechanism is not applicable to ultrafast ET. At the same time, both normal (when $\Delta G_{ET} < -0.3$ eV) and inverted (when $\Delta G_{ET} > -0.3$ eV) dependencies (Figure 6) are observed even though the identity of the mechanism contrary to the conclusion made by Mataga et al. that the "energy gap law seems to be affected by the change of the solvent polarity".[51] Actually, eq 12 predicts the transformation of positive slope to negative one at $\Delta E_{ET} = \lambda_V$. Thus, the transformation of normal to inverted dependence of k_{ET} on ΔE_{ET} (or ΔG_{ET}) does not need any change of the mechanism (similarly to the description of the emission spectra envelope by eq 2 when transition from rising branch to dropping branch occurs in the frame of one photophysical process). A quite different situation arises when ΔE_{ET} reaches zero and becomes negative ($\Delta G_{ET} > -\lambda_S$). Then, radiationless quantum transition mechanism vanishes and thermally activated medium reorganization becomes necessary for ET. Therefore, change of mechanism takes place, but it occurs at a substantially greater ΔG_{ET} (when ΔE_{ET} becomes negative) and the radiationless transition rate constant falls down below $1/\tau_L$. Still, normal dependence of k_{ET} vs ΔG_{ET} (or ΔE_{ET}) can be observed for both radiationless transition and thermally activated medium reorganization mechanisms in the ranges of $\lambda_V > \Delta E_{ET} > 0$ and $-\Delta G_{ET} < \lambda_S$, respectively. For very fast back ET, radiationless transitions normal region can be hidden by relatively slow medium relaxation in the process of the preparation of geminate radical ion pairs (see below).

It is quite important that medium and reactants reorganization affects differently primary charge separation and secondary charge recombination stages of radiationless ET (when $-\Delta G_{CS} > \lambda_S$ ($\Delta E_{CS} > 0$) and $-\Delta G_{CR} > \lambda_S$) in picosecond and nanosecond time domains ($k < 1/\tau_L$). The solvent shell of the initial ground state does not undergo substantial changes during photon absorption. For this reason, the energy gap ΔE_{CS} is low in sensitivity to the medium polarity and close to that in vacuum or, more precisely, in the medium with $\epsilon_S = n^2$ (for nonpolar ground and LE states). On the contrary, the energy of the polar CT state and the energy gap ΔE_{CR} for CT → G transition depend strongly on the reorganization energy due to medium relaxation. In the case of weak coupled pairs (solvent separated pairs, dyads, and triads with $V_{10} < 0.01$ eV), charge recombination is controlled by the energy gap $\Delta E_{CR} = -\Delta G_{CR} - \lambda_S$ when $-\Delta G_{CR} > \lambda_S$. For less exergonic charge recombination reactions, when $-\Delta G_{CR} < \lambda_S$, energy gap ΔE_{CR} becomes negative passing zero (when the CR rate constant reaches $10^{10}-10^{12}$ s^{-1} for $V_{10} = 0.001-0.01$ eV) during the medium relaxation. Thereby, in this region charge recombination occurs to be controlled by the medium relaxation rate ($1/\tau_L$) regardless of the radiationless transition mechanism. Indeed, only the inverted region was observed for charge recombination rates in geminate radical ion pairs formed upon ET quenching of cyanoaromatics by amines.[32] CR rate constants reach their maximum values (close to $1/\tau_L$ for MeCN) at $-\Delta G_{CR} \approx \lambda_S$ and do not change at a further decrease of $-\Delta G_{CR}$ (Figure 5, curve 1). But medium relaxation is slower than CR in the ultrafast transitions inherent in strong coupled D−A pairs (exciplexes, contact pairs, dyads, and triads with $V_{12} > 0.1$ eV). The absence of medium relaxation expands the energy gap ΔE_{CR} and thereby reduces the rate of CT → G transition.

All these results indicate the correctness of the radiationless transition approach for the description of IC as well as of ISC in exciplexes. Therefore, for the evaluation of rate constants of IC and ISC in exciplexes using eq 12, one needs to estimate energy gaps ΔE_{CR} and ΔE_{ST} and matrix elements V_{10} and V_{13}. Parameters σ, S, and $h\nu_V$ vary in a rather narrow range and affect k_{IC}' and k_{ISC}' less. For a rough estimation of exciplex lifetimes, one can use a correlation between $1/\tau_0'$ and log k_{IC}' that reflects a mean value of IC quantum yield in exciplexes $\log\varphi_{IC}' = -0.5 \pm 0.3$ (in the absence of heavy atoms).

Radiationless Transition and Preliminary Reorganization Mechanisms of CS in LP and TP of Reactants. It is reasonable to extend the consideration of the competition of radiationless transition and preliminary medium reorganization mechanisms in LP and TP to excited-state CS reactions. Physically distinct radiationless quantum transition (eq 12) and preliminary reorganization mechanisms of ET have different crucial parameters controlling their rate constants: matrix element coupling LE and CT states V_{12} and ΔE_{CS}^* for the former mechanism and $1/\tau_L$ (or V_{12}) and $\Delta G^{\ddagger}$ for the latter mechanism ($k_{CS} = k^0 \times \exp[-\Delta G^{\ddagger}/k_B T]$). It is reasonable to consider a transformation of CS mechanism with the change of ΔG_{CS}^* as a competition between these mechanisms in LP and TP of reactants. LP and TP have different distance between reactant molecules, electronic coupling matrix element, reorganization energies, and formation rate constants. According to the Franck−Condon principle, charge separation in LP and TP is expected to yield SSRIPs and exciplexes (or CRIPs), respectively.

Three competitive processes will be considered:

(1) Radiationless transition from LE into CT state in TP yielding exciplexes is expected in the strongly exergonic region ($\Delta E_{CS}^* > 0$).

2) Radiationless transition from LE into CT state in LP yielding SSRIPs in the moderately exergonic region ($\Delta E_{CS}^* > 0$, $-\Delta G_{CS}^* > \lambda_S$).

3) Thermally activated preliminary medium and reactants reorganization in LP (original Marcus model) yielding SSRIPs ($\Delta E_{CS}^* < 0$, $-\Delta G_{CS}^* < \lambda_S$).

Distinctions between these two kinds of reactant pairs and three mechanisms of ET are collected in Table 4.

Figure 8 presents cuts in the free-energy surfaces of reactants and products along a medium and reactant reorganization coordinate and illustrates the physical behavior of ΔE_{CS}^* and $\Delta G^{\ddagger}$ in loose and tight pairs and their dependence on ΔG_{CS}^*. Parabolas represent free energies of reactants and products for three above mentioned processes. Parabolas 1 and 2 represent the energies of LP and TP of the reactants, respectively, 3 and 4 represent the energies of SSRIP and CRIP, respectively, for the highly exergonic reaction ($\Delta G_{CS}^* = -1.7$ eV, $\Delta E_{CS}^* = 0.7$ eV), and 5 represents the energy of SSRIP for the isoergonic ($\Delta G_{CS}^* = 0$) reaction. The difference in reorganization energies for CRIP and SSRIP formation was discussed above. It is important to emphasize that the energy gap ΔE_{CS}^*(LP) is substantially smaller than ΔE_{CS}^*(TP) because of different electrostatic terms $(e^2/4\pi\epsilon_0)/n^2 r_{AD}$ for nonrelaxed SSRIP and CRIP formed as a result of Franck−Condon transitions. This difference reaches ca. 0.4 eV according to the aforementioned data of Gould et al.[45,46] for ion pairs and corresponds to the difference in r_{AD} between CRIP and SSRIP (ca. 0.2 nm). At the same time, the electronic coupling matrix element V_{12} for ET in TP is ca. 10−100 times greater than that in LP providing substantially higher rate constants for radiationless ET in tight pairs regardless of greater ΔE_{CS}^*.

TABLE 4: Behavior of Radiationless Quantum Transition and Preliminary Thermally Activated Reorganization Mechanisms of Excited-state ET (Photoinduced Charge Separation and Charge Shift) and Back ET in Geminate Radical Ion Pairs (Charge Recombination and Charge Shift)

	Mechanism		
	radiationless quantum transition (medium and reactants reorganization after ET)		preliminary thermally activated reorganization (medium and reactants reorganization before ET)
	tight pairs	loose pairs	loose pairs
energy gap	$\Delta E_{CS}^* = -(\Delta G_{ET}^* + \lambda_S')$; $\Delta E_{CR} = \Delta G_{ET} - \lambda_S'$	$\Delta E_{CS}^* = -(\Delta G_{ET}^* + \lambda_S)$; $\Delta E_{CR} = \Delta G_{ET} - \lambda_S$	
r_{AD}/nm	0.3 − 0.5	0.8 − 1.2	0.8 − 1.2
λ_S (λ_S')/eV[a]	0.3 − 0.5	0.8 − 1.5	0.8 − 1.5
V_{12}/eV	0.01 − 0.4	0.001 − 0.01	0.001 − 0.01
	Monomolecular Reactions (ET Rate Control) Photoexcitation of Ground-State CT Complexes or Reactants Pairs and Back ET in Geminate Radical Ion Pairs (Charge Recombination and Shift)		
attributes	k_{ET} (TP) > k_{ET} (LP)	k_{ET} (TP) > k_{ET} (LP)	$k_{ET} < 1/\tau_L$ ($\approx 10^{12}$ s^{-1} [a])
requirements	$\Delta G_{CS}^* < -\lambda_S$; $\Delta G_{CR} < -\lambda_S$	$\Delta G_{CS}^* < -\lambda_S$; $\Delta G_{CR} < -\lambda_S$	$\Delta G_{CS}^* > -\lambda_S$; $\Delta G_{CR} > -\lambda_S$
	Bimolecular Reactions (ET Rate and/or Diffusion Control) Excited-State ET (Photoinduced Charge Separation and Shift)		
requirements	k_{CS}(LP) < k_{Sep}(LP)	k_{Sep}(LP) < k_{CS}(LP)	
	$\Delta G_{CS}^* < -2$ eV	-2 eV < $\Delta G_{CS}^* < -\lambda_S$	$\Delta G_{CS}^* > -\lambda_S$

[a] Evaluations of λ_S and λ_S' are given for polar ($\epsilon_S = 20-40$) solvents.

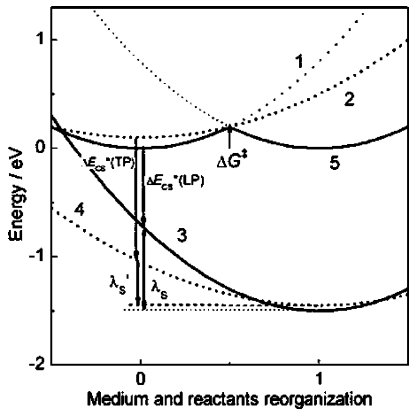

Figure 8. Schematic diagram of free-energy surfaces of reactants (line 1, LP; line 2, TP) and products (line 3, SSRIP; line 4, CRIP) along a medium and reactant reorganization coordinate for exergonic ET reactions ($\Delta E_{CS}^* > 0$, $-\Delta G_{CS}^* > \lambda_S$). Curve 5 is the energy of SSRIP for isoergonic reaction ($\Delta G_{CS}^* = 0$, $\Delta E_{CS}^* < 0$).

Figure 9a shows simulated dependences of free energies of LE state (1), Franck−Condon SSRIP (2) ($\Delta G_{CS}^* + \lambda_S$) and CRIP (3) ($\Delta G_{CS}^* + \lambda'_S$) states, relaxed SSRIP (4) (= ΔG_{CS}^*), and the activation energy (5) of preliminary thermally activated charge separation in LP on ΔG_{CS}^* and ΔE_{CS}^* in polar solvents for $\lambda_S = 0.8$ and $\lambda'_S = 0.4$ eV. The dependences of electron-transfer rate constants on ΔG_{CS}^* can be considered using this energy diagram. Dash lines 6 and 7 in Figure 9b ($\Delta E_{CS}^* > 0$) correspond to monomolecular radiationless transition rate constants in TP and LP, respectively, in accordance with eq 12 for $V_{12} = 0.2$ and 0.002 eV in TP and LP, respectively. In the whole range of $\Delta E_{CS}^* > 0$, monomolecular rate constants of radiationless ET in tight pairs are 2.5−3.5 order higher than in LP. Monomolecular rate constants for radiationless CS exceed those for preliminary thermally activated monomolecular CS in LP (dash line 8) when $\Delta E_{CS}^* > 0$. But the latter dominates when $\Delta E_{CS}^* < 0$ and the radiationless mechanism vanishes. The preexponential factor for preliminary thermally activated CS is equal to the least of the two following values: $(1/\tau_L)$ or $(4\pi^2/h)V_{12}^2(4\pi k_B T\lambda)^{-1/2}$, where τ_L varies in the range 0.3−10 ps for low viscous solvents. Electronic coupling controls CS rate in loose pairs with $V_{12} < 0.01$.

The bimolecular quenching rate constant in solution can be expressed as a function of rate constants of monomolecular CS, k_{CS}, and rate constants of formation, k_{Diff}, and separation, k_{Sep}, of LP and TP

$$k_Q = k_{Diff}/[1 + (k_{Sep}/k_{CS})] \quad (15)$$

where k_{Diff} and k_{Sep} are controlled by diffusion. Rate constants of the formation of LP and TP can be estimated using the Stokes−Einstein equation as

$$k_{Diff} \approx (k_B T/2.5\eta)(2r_{AD}/\rho_{A(D)}) = (2r_{AD}/\rho_{A(D)})[(3.26 \times 10^4)T]/(\eta/\mathrm{P})\ \mathrm{dm^3\ mol^{-1}\ s^{-1}} \quad (16)$$

where η is viscosity (in Poise). For LP, $r_{AD}/\rho_{A(D)} \approx 3-5$, and for TP $r_{AD}/\rho_{A(D)} \approx 1.5-2$. In acetonitrile ($\eta = 0.35$ cP at 298 K), the formation rate constant for LP and TP are 2×10^{10} dm^3 mol^{-1} s^{-1} and 1×10^{10} dm^3 mol^{-1} s^{-1}, respectively. The former value coincides well with common evaluation for diffusion rate constant by Debye equation $k_{Diff} = 8RT/3000\eta = 2.22 \times 10^5 (T/\eta) = 1.9 \times 10^{10}$ dm^3 mol^{-1} s^{-1}. The rate constant for the conversion of LP into TP is ca. 2×10^{10} s^{-1} and the rate constant for the conversion of TP into LP is ca. 1×10^{10} s^{-1}. Hence, k_{Sep} (TP) = 4×10^{10} and k_{Sep} (LP) = 1×10^{10} s^{-1} in acetonitrile at room temperature.

The quenching rate constants are presented in Figure 9b by solid lines for radiationless mechanism in TP (line 9) and LP (line 10), and for thermally activated preliminary reorganization mechanism in LP (line 11). The radiationless mechanism in TP dominates over the same mechanism in LP when k_{CS}(LP) < k_{Sep} (LP) (ΔG_{CS}^* < ca. −1.5 eV) and the inverted region can be observed only when k_{CS}(TP) < k_{Sep} (TP) (ΔG_{CS}^* < ca. −2.5 eV). The thermally activated preliminary reorganization mechanism in LP dominates when $-\Delta G_{CS}^* < \lambda_S$ but is hidden under the diffusion controlled limit. In a general case, the ratio of charge separation and diffusion rates controls the conversion of one mechanism into another.

Different primary products should be formed in different ranges of ΔG_{CS}^* according to discussed interplay of CS mechanisms in LP and TP of reactants. In contrast to the common suggestion that SSRIPs are formed in exergonic

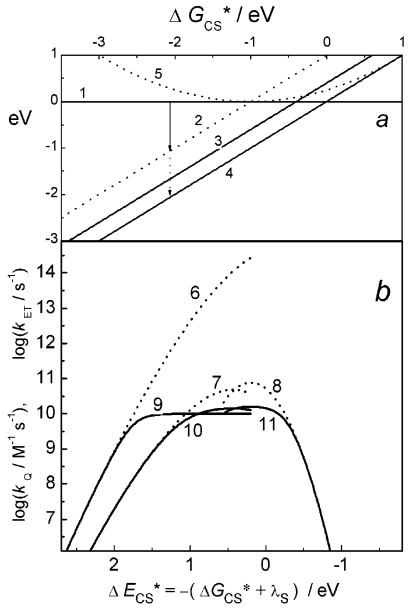

Figure 9. (a) Simulated dependences of free energies of LE state (line 1), Franck−Condon SSRIP (line 2) and CRIP (line 3) states, relaxed SSRIP (line 4), and activation energy $\Delta G^{\ddagger}$ (line 5) on ΔG_{CS}* and ΔE_{CS}* for polar solvents ($\lambda_S = 0.8$ eV, $\lambda_S' = 0.4$ eV). (b) The dependence of ET rate constants ($V_{12} = 0.2$ and 0.002 eV for CRIPs and SSRIPs, respectively) on ΔG_{CS}* and ΔE_{CS}* for: monomolecular ET according to radiationless transition mechanism in TP (line 6) and LP (line 7) and according to preliminary thermally activated mechanism in LP (line 8); bimolecular ET according to radiationless transition mechanism in TP (line 9) and LP (line 10) and according to preliminary thermally activated mechanism in LP (line 11).

reactions because of the large distance of CS (1.0 − 1.4 nm), one can expect the formation of CRIPs in strongly exergonic reactions (ΔG_{CS}* < −1.5 eV) because of much faster CS in TP relative to LP of reactants. This is confirmed by experimental results of Vauthey et al.[49] who observed the formation of CRIPs in the reaction of excited perylene with tetracyanoethylene (ΔG_{CS}* = −2.2 eV).

Different kinds of the dependencies of logk_{CS} vs ΔG_{CS}* are inherent in radiationless and medium reorganization mechanisms of ET. The radiationless mechanism yields inverted dependence of k_{CS} on ΔE_{CS}* when ΔE_{CS}* > $h\nu_V$. Only at 0 < ΔE_{CS}* < $h\nu_V$, flat or rather weak positive dependence can be observed. At negative ΔE_{CS}*, the radiationless mechanism vanishes and only normal dependence related to the medium and reactants reorganization can be observed. Above all, the discussion of normal and inverted dependence of k_{CS} on ΔE_{CS}* or ΔG_{CS}* should take into account the important distinctions of monomolecular and bimolecular CS reactions related to the diffusion of reactants. The rate of monomolecular CS reactions in single molecules, complexes, dyads or triads, and contact or solvent separated pairs is controlled only by the behavior of CS mechanism: when $-\Delta G_{CS}$* > λ_S and ΔE_{CS}* > 0 the reaction follows the radiationless transition mechanism and inverted dependence is observed easily. The radiationless mechanism operates in the whole range of ΔG_{CS}* and both "inverted" and "normal" wings can be observed[21−23] when the radiationless transition rate constant is greater than the reciprocal longitudinal relaxation time of the medium $\tau_L = (n^2/\epsilon)\tau_D$ (ultrafast CS or reactions in very viscous or glassy medium) where τ_D is Debye relaxation time. On the other hand, in second-order CS reactions a competition of CS in initially formed LP with its conversion into TP becomes the main factor controlling the mechanism and the nature of the dependence of k_{CS} on ΔE_{CS}* or ΔG_{CS}*. Normal dependence is easily observed in all second-order ET reactions. But observation of inverted dependence is difficult because this dependence is hidden under the diffusion controlled limit down to ΔG_{CS}* = −(2.5−3) eV because of very fast CS in TP (up to $10^{12}-10^{14}$ s^{-1} even for ΔE_{CS}* > 3 eV). Apparently, fast internal conversion in TP can cause the lack of the inverted region for strongly exergonic CS even in the absence of other factors such as formation of electronically excited radical ions, partial dielectric saturation, etc. Similarly, the absence of the inverted region for ΔG_{CS}* > −(2.5 −3) eV arises from a model of continuous dependence of parameters V_{12}, ΔG_{CS}*, λ_S, and k^0 on the distance between reactant molecules r_{AD} considered by Mataga et al.[52]

Conclusions

The physically correct application of the radiationless quantum transition mechanism to IC and ISC in exciplexes (charge recombination) requires the use of the energy gap ΔE_{CR} and the spectral width of vibronic levels σ rather than thermodynamic quantities ΔG_{CR} and λ_S (which imply the equilibrium initial and final states). All arguments[9] for practical advantages of using free energy surfaces instead of potential energy surfaces fail because quantum transitions follow the Franck−Condon principle and yield nonequilibrium states. No reorganization of the medium and the reactants occurs during quantum transition. No direct and universal relation of ΔE_{CR} with ΔG_{CR} exists because λ_S depends substantially on the nature of the reactant pairs (ca. 0.3−0.5 eV for TP and 0.8−1.5 eV for LP in polar solvents). Common use of eq 13, which artificially combines these mechanisms, is misleading and may result in erroneous conclusions because the physical behavior of radiationless quantum transition mechanism is completely different from thermally activated preliminary reorganization (Marcus) mechanism. The use of free energy surfaces is still reasonable for relatively slow preliminary medium and reactants reorganization, which provides conditions for ET by the shift of energy levels of initial and final states.

Exciplex emission spectra (eq 2) and the dependence of IC rate constants on the energy gap (eq 12) are described by the same values of parameters S, σ, and $h\nu_V$. This verifies radiationless quantum transition mechanism of charge recombination (IC and ISC) in exciplexes. Envelopes of exciplex emission spectra as well as rates of internal conversion and intersystem crossing are governed by inhomogeneous broadening σ rather than by reorganization energy λ_S. Experimental data reveal a very small temperature effect on exciplex decay lifetimes (activation enthalpy less than 1−5 kJ mol^{-1})[53,54] thereby confirming activationless quantum transition mechanism of exciplex decay. Parameters $h\nu_V$, σ, S, and λ_V have practically the same values for exciplexes and SSRIP suggesting that dominant accepting vibrational modes for these species are identical. On the contrary, the value of V_{10} for charge recombination in exciplexes and in CRIPs substantially exceeds that for SSRIPs (0.01−0.2 and 0.001−0.003 eV, respectively) reflecting the exponential decay of V_{10} with the distance. The absence of the normal region for charge recombination in exciplexes and CRIPs contrary to SSRIPs is caused by a much smaller value of λ_S.

The relatively long lifetimes of experimentally studied exciplexes are caused by a rather large energy gap for CR (exciplex emission maxima are in the range 500−800 nm, which corresponds to ΔE_{CR} = 1.5−2.5 eV) regardless of the high value of the electronic coupling matrix element. From this viewpoint, back ET (internal conversion and intersystem crossing) in exciplexes and CRIPs are closer to ordinary radiationless

transition rather than to ET reaction, in contrast to back ET in SSRIPs in which λ_S is substantially greater.

Ultrafast CS reactions ($k_{CS} > 1/\tau_L$) follow the radiationless quantum transition mechanism and demonstrate both normal and inverted dependence of k_{CS} on ΔE_{CS}* depending on the value of ΔE_{CS}* (normal dependence for $\Delta E_{CS}^* < \lambda_V = S\,h\nu_V$ and inverted dependence for $\Delta E_{CS}^* > \lambda_V$). Thereby, the transition from the normal to inverted region does not give any evidence for the change of the reaction mechanism. The use of ΔG_{CS} and λ_S for ultrafast ET is misleading and may result in erroneous conclusions because CS precedes the medium and the reactants reorganization and cannot be influenced by them.

The quantity ΔE_{CR} can be time dependent when GRIP is generated by excited-state CS reaction or by direct excitation of ground-state CT complex because of medium relaxation processes (ca. 0.3−10 ps). This can affect CR kinetics and can cause nonexponential decay of GRIP accelerating this decay because of the gradual decrease of ΔE_{CR} during the relaxation.

The interplay of quantum transition and preliminary reorganization mechanisms of charge separation in LP and TP builds up the main features of charge separation reactions. (1) Strong coupling in TP (ca. 0.1−0.4 eV) provides very large values of k_{CS} which exceed k_{Sep} for these pairs and maintains diffusion control of the second-order excited-state quenching and the absence of inverted dependence of k_Q vs ΔG_{CS}* down to $\Delta G_{CS}^* < -3.0$ eV. This is the most general mechanism providing the lack of inverted region in excited-state charge separation reactions even in the absence of other factors. Because of the Franck−Condon principle, these reactions yield CRIPs. (2) Less exergonic CS reactions ($\Delta G_{CS}^* > -2.0$ eV) occur in LP and yield SSRIPs because of faster rates of LP relative to TP formation. (3) The radiationless transition mechanism fails at a further increase of ΔG_{CS}* and the thermally activated preliminary reorganization (Marcus) mechanism appears when $\Delta G_{CS}^* > -\lambda_S$ ($\Delta E_{CS}^* < 0$) and yields SSRIPs.

The difference between charge separation reactions (with absence of inverted dependence) and charge recombination reactions (with clear observed inverted dependence) can be attributed mainly to the difference in the orders of these reactions. Indeed, charge separation is studied usually for bimolecular reactions between uncharged reactants molecules (at least one of the reactants is uncharged) and controlled by their diffusion. On the contrary, charge recombination is studied predominantly in solvent separated or contact radical ion pairs generated by preliminary excited-state charge separation reactions. In this case, radiationless rate constants can reach 10^{12}−10^{14} s^{-1} and are controlled mainly by V_{10} and ΔE_{CR} values with typical inverted dependence.

Acknowledgment. The work was supported by the Russian Foundation for Basic Research, Project No. 05-03-32554.

References and Notes

(1) Kuzmin, M. G. *Pure Appl. Chem.* **1993**, *65*, 1653.
(2) Kuzmin, M. G. *J. Photochem. Photobiol. A* **1996**, *102*, 51.
(3) Grosso, V. N.; Chesta, C. A.; Previtali, C. M. *J. Photochem. Photobiol., A* **1997**, *118*, 157.
(4) Jacques, P.; Allonas, X.; von Raumer, M.; Suppan, P.; Haselbach, E. *J. Photochem. Photobiol., A* **1997**, *111*, 41.
(5) Hubig, S. M.; Kochi, J. K. *J. Am. Chem. Soc.* **1999**, *121*, 1688.
(6) Iwai, S.; Murata, S.; Katoh, R.; Tachiya, M.; Kikuchi, K.; Takahashi, Y. *J. Chem. Phys.* **2000**, *112*, 7111.
(7) Kuzmin, M. G.; Soboleva, I. V.; Dolotova, E. V.; Dogadkin, D. N. *Photochem. Photobiol. Sci.* **2003**, *2*, 967.
(8) Kuzmin, M. G.; Soboleva, I. V.; Dolotova, E. V. *High Energy Chem.* **2006**, *40* (4), 234.
(9) Marcus, R. A. *J. Phys Chem.* **1989**, *93*, 3078.
(10) Vauthey, E.; Phillips, D. *Chem. Phys.* **1990**, *147*, 421.
(11) Gould, I. R.; Boiani, J. A.; Gaillard, E. B.; Googman, J. L.; Farid, S. *J. Phys. Chem. A.* **2003**, *107*, 3515.
(12) Marcus, R. A. *J. Phys. Chem.* **1956**, *24*, 966.
(13) Jortner, J.; Rice, S. A.; Hochstrasser, R. M. *Adv. Photochem.* **1969**, *7*, 149.
(14) Kjaer, A. M.; Ulstrup J. *J. Am. Chem. Soc.* **1987**, *109*, 1934.
(15) Marcus, R. A. *J. Chem. Phys.* **1984**, *81*, 4494.
(16) Burshtein, A. I. *Adv. Chem. Phys.* **2000**, *114*, 419.
(17) Barzykin, A. V.; Frantsuzov, P. A.; Seki, K.; Tachiya, M. *Adv. Chem. Phys.* **2002**, *123*, 511.
(18) Miller, L. R.; Calcaterra, L. T.; Closs, G. L. *J. Am. Chem. Soc.* **1984**, *106*, 3047.
(19) Wasielewski, M. R.; Niemczyk, N. P.; Svec, W. A.; Pewitt, E. B. *J. Am. Chem. Soc.* **1985**, *107*, 1080.
(20) Irvine, M. P.; Harrison, R. J.; Beddard, G. S.; Leighton, P.; Sanders, J. K. M. *Chem. Phys.* **1986**, *104*, 315.
(21) Ohno, Y.; Yoshimura, A.; Shioyama, H.; Mataga, N. *J. Phys. Chem.* **1987**, *91*, 4365.
(22) Gould, I. R.; Ege, D.; Mattes, S. L.; Farid, S. *J. Am. Chem. Soc.* **1987**, *109*, 5057.
(23) Mataga, N.; Asahi, T.; Kanda, Y.; Okada, T.; Kakitani, T. *Chem. Phys.* **1988**, *127*, 249.
(24) Vauthey, E.; Suppan, P.; Haselbach, E. *Helv. Chim. Acta.* **1988**, *71*, 93.
(25) Levin, P. P.; Pluzhnikov, P. F.; Kuzmin, V. A. *Chem. Phys. Lett.* **1988**, *127*, 249.
(26) Chen, P.; Duesing, R.; Tapolsky, G.; Meyer, T. J. *J. Am. Chem. Soc.* **1989**, *111*, 8305.
(27) Gould, I. R.; Ege, D.; Moser, J. E.; Farid, S. *J. Am. Chem. Soc.* **1990**, *112*, 4290.
(28) Kikuchi, K.; Takahashi, I.; Hoshi, M.; Niwa, T.; Katagiri, T.; Miyashi, T. *J. Phys. Chem.* **1991**, *95*, 2378.
(29) Suppan, P. *Top. Curr. Chem.* **1992**, *63*, 95.
(30) Asahi, T.; Ohkohchi, M.; Mataga, N. *J. Phys. Chem.* **1993**, *97*, 13132.
(31) Gould, I. R.; Noukakis, D.; Gomes-Jahn, L.; Young, R. H.; Goodman, J. L.; Farid, S. *Chem. Phys.* **1993**, *176*, 439.
(32) Vauthey, E. *J. Phys. Chem. A* **2001**, *105*, 340.
(33) Dogadkin, D. N.; Soboleva, I. V.; Kuzmin, M. G. *High Energy Chem.* **2001**, *35* (2), 107.
(34) Dogadkin, D. N.; Dolotova, E. V.; Soboleva, I. V.; Kuzmin, M. G.; Plyusnin, V. F.; Pozdnyakov, I. P.; Grivin, V. P.; Phillips, D.; Murphy, K. *High Energy Chem.* **2004**, *38* (6), 386.
(35) Dogadkin, D. N.; Dolotova, E. V.; Soboleva, I. V.; Kuzmin, M. G.; Plyusnin, V. F.; Pozdnyakov, I. P.; Grivin, V. P.; Vauthey, E.; Brodard, P.; Nicolet, O. *High Energy Chem.* **2004**, *38* (6), 392.
(36) Dolotova, E.; Dogadkin, D.; Soboleva, I.; Kuzmin, M.; Nicolet, O.; Vauthey, E. *Chem. Phys. Lett.* **2003**, *380*, 729.
(37) Kuzmin, M. G.; Dolotova, E. V.; Soboleva, I. V. *Russ. J. Phys. Chem.* **2002**, *76*, 1109.
(38) Huang, K.; Rhys, A. *Proc. R. Soc. London, Ser. A* **1950**, *204*, 406.
(39) Levy, D.; Arnold, B. R. *J. Phys. Chem. A* **2005**, *109*, 8572.
(40) Kuzmin, M. G. *Russ. J. Phys. Chem.* **1999**, *73*, 1625.
(41) Kuzmin, M. G.; Soboleva, I. V. *Russ. J. Phys. Chem.* **2001**, *75*, 408.
(42) Weller, A. *Pure Appl. Chem.* **1982**, *54*, 1885.
(43) Gould, I. R.; Young, R. H.; Mueller, L. J.; Albrecht, A. C.; Farid, S. *J. Am. Chem. Soc.* **1994**, *116*, 8188.
(44) Mataga, N.; Okada, T.; Yamamoto, N. *Bull. Chem. Soc. Jpn.* **1966**, *39*, 2562.
(45) Arnold, B. R.; Noukakis, D.; Farid, S.; Goodman, J. L.; Gould, I. R. *J. Am. Chem. Soc.* **1995**, *117*, 4399.
(46) Arnold, B. R.; Farid, S.; Goodman, J. L.; Gould, I. R. *J. Am. Chem. Soc.* **1996**, *118*, 5482.
(47) Asahi, T.; Mataga, N. *J. Phys. Chem.* **1991**, *95*, 1956.
(48) Morandeira, A.; Fürtenberg, A.; Gumy, J.-C.; Vauthey, E. *J. Phys. Chem. A* **2003**, *107*, 5375.
(49) Pagès, S.; Lang, B.; Vauthey, E. *J. Phys. Chem. A* **2004**, *108*, 549.
(50) Nicolet, O.; Banerji, N.; Pagès, S.; Vauthey, E. *J. Phys. Chem. A* **2005**, *109*, 8236.
(51) Mataga, N.; Taniguchi, S.; Chosrowjan, H.; Osuka, A.; Yoshida, N. *Chem. Phys.* **2003**, *295*, 215.
(52) Kakitani, T.; Matsuda, N.; Yoshimori, A.; Mataga, N. *Prog. React. Kinet.* **1995**, *20*, 347.
(53) Dolotova, E. V.; Soboleva, I. V.; Kuzmin, M. G. *High Energy Chem.* **2003**, *37* (4), 231.
(54) Dogadkin, D. N.; Dolotova, E. V.; Soboleva, I. V.; Kuzmin, M. G.; Plyusnin, V. F.; Pozdnyakov, I. P.; Grivin, V. P. *High Energy Chem.* **2005**, *39* (1), 20.